

The effects of seeing on Sèrsic profiles

I. Trujillo,¹ J. A. L. Aguerri,^{2*} J. Cepa¹ and C. M. Gutiérrez¹

¹*Instituto de Astrofísica de Canarias, E-38205 La Laguna, Tenerife, Spain*

²*Astronomisches Institut der Universität Basel, Venusstrasse 7, CH-4102 Binningen, Switzerland*

Accepted 2000 August 29. Received 2000 July 24; in original form 2000 April 28

ABSTRACT

The effects of seeing on the parameters of the Sèrsic profile are studied in an analytical form using a Gaussian point spread function. The surface brightness of Sèrsic profiles is proportional (in magnitudes) to $r^{1/n}$. The parameter n serves to classify the type of profile and is related to the central luminosity concentration. It is the parameter most affected by seeing; furthermore, the value of n that can be measured is always smaller than the real one. It is shown that the luminosity density of the Sèrsic profile with n less than 0.5 has a central depression, which is physically unlikely. Also, the intrinsic ellipticity of the sources has been taken into account and we show that the parameters are dependent when the effects of seeing are non-negligible. Finally, a prescription for correcting raw effective radii, central intensities and n parameters is given.

Key words: atmospheric effects – methods: data analysis – galaxies: distances and redshifts – galaxies: photometry.

1 INTRODUCTION

Galaxies exhibit many different morphologies and therefore dynamical properties. They also vary enormously in size and luminosity. Galaxies can consist of one or more dynamical substructures. The classification methods are mainly based on the morphologies of these substructures. The most widely used classification scheme is that introduced by Hubble (1936), which is based on the ratio of the spheroidal bulge and disc luminosities. The galactic morphological types vary from ellipticals (with only spheroidal components) to late-type spirals, with small spheroids and prominent disc components. Irregular galaxies, which are later than spirals in the Hubble sequence, are characterized by the absence of symmetry. In recent decades much work has been done to improve the method for determining the principal components of galaxies (e.g. Prieto et al. 2000 and references therein).

It is usually assumed that the light of a galaxy follows the mass distribution. The mass distribution can then be inferred by modelling the light distribution. The light of a galaxy is usually modelled by fitting the surface brightness profile of each structural component with certain analytical curves. These laws have certain free parameters that must be determined during the fitting process. From de Vaucouleurs (1948), it is well known that the surface brightness profile (in magnitudes) of elliptical galaxies is proportional to $r^{1/4}$ (where r is the radial distance to the centre of the galaxy). This law was also applied to bulges of spiral galaxies that have similar shapes, colours and kinematics to those of ellipticals. It has recently been discovered that not all bulges follow an $r^{1/4}$ profile (Caon, Capaccioli & D’Onofrio 1993; Andredakis, Peletier

& Balcells 1995). A better analytical form is the Sèrsic profile (Sèrsic 1968) which has surface brightness proportional to $r^{1/n}$ and generalizes the $r^{1/4}$ law. The parameter n is one of the three free parameters and it defines the type of the profile. When $n = 1$ the surface brightness profile is exponential. Increasing values of n give more centrally concentrated luminosity profiles. Andredakis et al. (1995) found a correlation between the value of n and the morphological type of the galaxies, in the sense that early types show larger values of n than do late-type galaxies. Exponential profiles have been used extensively in order to fit the surface brightness profiles of discs of spiral galaxies. Sèrsic profiles have also been used in other types of galaxies; for example, Davies et al. (1988) propose that dwarf ellipticals are well fitted with a Sèrsic law with $n \leq 2$.

Ground-based astronomical images are always affected by atmospheric blurring. Many papers have been written on the subject and much effort has been invested in the construction of new optics to minimize its effects. Seeing scatters light from the inner, centrally concentrated core to the outer, more diffuse regions of galaxies, producing a mean surface brightness lower than the true values and larger effective radii. These effects can change the results of the photometric parameters obtained from the fits of the observed surface brightness profiles; moreover, the dynamical properties inferred from these parameters will also be wrong. Although seeing affects all points in a galaxy, its effects are more important in the central regions. Seeing effects were studied extensively in the case of elliptical galaxies with $r^{1/4}$ profiles (Franx, Illingworth & Heckman 1989; Saglia et al. 1993). These authors showed that the effects of seeing on the photometric properties of elliptical galaxies can extend as far as five seeing discs.

* E-mail: jalfonso@astro.unibas.ch

Saglia et al. (1993) also showed that seeing effects become important for distant ellipticals ($cz > 8000 \text{ km s}^{-1}$). They found that uncorrected fundamental plane distances are systematically too high if seeing effects are not taken into account. This is caused by the small angular size of the objects at great distances: for a flat universe with $H_0 = 75 \text{ km s}^{-1} \text{ Mpc}^{-1}$, an object at 30 kpc has an angular size of 15 arcsec^2 at $z = 0.1$ and 3 arcsec^2 at $z = 0.5$. This means that a typical seeing of 1 arcsec^2 is equivalent to 1/15 of the size of the object at $z = 0.1$, but is 1/3 of the object at $z = 0.5$. The seeing will therefore produce important effects on these objects at large radii. Thus, the study of the effects of seeing on surface brightness profiles must be taken into account when the photometric parameters of these galaxies are obtained from the decomposition of their surface brightness profiles. The new generation of ground-based telescopes and the study of galaxies at higher redshifts make these kinds of studies very important.

In this paper we present an analytical treatment of seeing effects on Sèrsic profiles, taking into account the ellipticity of the objects. The mathematical treatment of seeing will be given in Section 2. In Section 3 we present the effect of the seeing on the photometric parameters. An easy prescription for correcting the parameters measured from the raw profiles is given in Section 4. The analysis of these results is given in Section 5.

2 MATHEMATICAL ANALYSIS

The blurring of images by the atmosphere and imperfections in telescope optics (seeing) degrades measurements of the surface brightnesses of galaxies. The seeing is characterized by the point spread function (PSF). The PSF gives the probability that a photon will hit the imaging device at a point different from where it would have hit in the absence of seeing. This can be determined observationally by studying the scattering of stellar light. PSFs are well described by Gaussian functions, Gaussian functions with exponential wings, linear superpositions of Gaussian functions, Moffat functions, etc. (e.g. Moffat 1969; King 1971; Schweizer 1979). Among these analytical approximations of PSFs, the most widely used is the single Gaussian. The main goal of the present paper is to evaluate the effects of seeing on the parameters of Sèrsic profiles in a completely analytical form and to take into account the ellipticity of the surfaces brightness distribution in this treatment. We develop our analysis using a Gaussian PSF and in Section 5 we shall compare this with a different PSF.

Assume a circular Gaussian function of dispersion σ to model the point spread function:

$$\text{PSF}(r) = \frac{1}{2\pi\sigma^2} \exp\left[-\frac{1}{2}\left(\frac{r}{\sigma}\right)^2\right]. \quad (1)$$

Consider a case where, in the absence of seeing, the surface brightness distribution $I(\mathbf{r})$ of the galaxy is elliptically symmetric. This means that the isophotes of the object all have the same constant ellipticity ϵ ($\epsilon = 1 - b/a$, where a and b are the semi-major and semiminor axes, respectively, of the isophote).

Elliptical coordinates (ξ, θ) are the most appropriate for our problem and are defined as

$$\begin{aligned} x &= \xi \cos \theta \\ y &= \xi(1 - \epsilon) \sin \theta. \end{aligned} \quad (2)$$

In this coordinate system, the surface brightness distribution, $I(\mathbf{r})$, of an elliptical source depends only on ξ : $I(\mathbf{r}) = I(\xi)$. The convolution equation that represents the effect of seeing on the

surface brightness distribution is given by

$$I_c(\xi, \theta) = (1 - \epsilon) \int_0^\infty \xi' d\xi' \int_0^{2\pi} d\theta' \text{PSF}(\xi', \theta', \xi, \theta) I(\xi'), \quad (3)$$

where $\text{PSF}(\xi', \theta', \xi, \theta)$ is the Gaussian PSF given by

$$\begin{aligned} \text{PSF}(\xi', \theta', \xi, \theta) &= \frac{1}{2\pi\sigma^2} \exp\left(-\frac{1}{2} \frac{\xi'^2 + \xi^2}{\sigma^2}\right) \\ &\times \exp\left(\frac{\xi\xi' \cos(\theta + \theta')}{\sigma^2}\right) \\ &\times \exp\left[-\frac{(\epsilon^2 - 2\epsilon)(\xi' \sin \theta' - \xi \sin \theta)^2}{2\sigma^2}\right]. \end{aligned} \quad (4)$$

2.1 Analytical convolution of Sèrsic profiles

In the particular case of Sèrsic profiles, the surface brightness distribution is given by

$$I(\xi) = I(0) \exp\left[-\left(\frac{\xi}{r_0}\right)^{1/n}\right], \quad (5)$$

where $I(0)$ is the central intensity and r_0 is the scalelength of the profile. Over the major axis of the object, $\theta = 0$, the analytical solution of equation (3) for this type of profile can be written as

$$\begin{aligned} I_c(\xi, 0) &= \frac{I(0)}{\pi^{1/2}} (1 - \epsilon) \exp\left[-\frac{1}{2}\left(\frac{\xi}{\sigma}\right)^2\right] \sum_{k=0}^{\infty} \frac{(-)^k}{k!} \\ &\times \left(\frac{\sqrt{2}\sigma}{r_0}\right)^{k/n} \times \sum_{l=0}^{\infty} \frac{1}{l!} (2\epsilon - \epsilon^2)^l \\ &\times \frac{\Gamma\left(l + \frac{1}{2}\right)}{\Gamma(l+1)} \Gamma\left(l + 1 + \frac{k}{2n}\right) \\ &\times M\left(l + 1 + \frac{k}{2n}, l + 1, \frac{1}{2}\left(\frac{\xi}{\sigma}\right)^2\right), \end{aligned} \quad (6)$$

where $M(\mu, \nu, z)$ are the confluent hypergeometric functions (Abramowitz & Stegun 1964, p. 504). This expression simplifies if the object is circular:

$$\begin{aligned} I_c(\xi) &= I(0) \exp\left[-\frac{1}{2}\left(\frac{\xi}{\sigma}\right)^2\right] \sum_{k=0}^{\infty} \frac{(-)^k}{k!} \\ &\times \left(\frac{\sqrt{2}\sigma}{r_0}\right)^{k/n} \Gamma\left(1 + \frac{k}{2n}\right) M\left(1 + \frac{k}{2n}, 1, \frac{1}{2}\left(\frac{\xi}{\sigma}\right)^2\right). \end{aligned} \quad (7)$$

In the limiting cases, $\xi \rightarrow \infty$ or $\sigma \rightarrow 0$, the asymptotic expression of the confluent hypergeometric function (Abramowitz & Stegun 1964, p. 504) can be used to recover the original Sèrsic expression:

$$I_c(\xi, 0) = I(0) \exp\left[-\left(\frac{\xi}{r_0}\right)^{1/n}\right] \left\{1 + O\left[\left(\frac{\xi^2}{2\sigma^2}\right)^{-1}\right]\right\}, \quad (8)$$

where $(\xi^2/2\sigma^2)^{-1}$ quantifies the differences between the Sèrsic profiles unaffected and affected by seeing in those asymptotic limits.

2.2 The effect of seeing on the ellipticity of the isophotes

In the absence of seeing, by construction, all isophotes of the Sèrsic profile have the same ellipticity, whereas the presence of seeing tends to make them circular. Using the isophote condition, $I(\xi, 0) = I(\xi, \pi/2)$ – the expression over the minor axis is written in appendix A – it is possible to derive an implicit equation that gives the variation of the ellipticity with the radial distance:

$$\epsilon(\xi) = 1 - \left[-2 \left(\frac{\sigma}{\xi} \right)^2 \ln f(\epsilon, \sigma^2, n, r_0, \xi, \epsilon(\xi)) \right]^{1/2}, \quad (9)$$

where f is given by:

$$\begin{aligned} f(\epsilon, \sigma^2, n, r_0, \xi, \epsilon(\xi)) &= \sigma^2 \exp \left[-\frac{1}{2} \left(\frac{\xi}{\sigma} \right)^2 \right] \sum_{k=0}^{\infty} \frac{(-)^k}{k!} \left(\frac{\sqrt{2}\sigma}{r_0} \right)^{k/n} \\ &\times \sum_{l=0}^{\infty} \frac{1}{l!} (2\epsilon - \epsilon^2)^l \frac{\Gamma(l + \frac{1}{2})}{\Gamma(l + 1)} \Gamma\left(l + 1 + \frac{k}{2n}\right) \\ &\times M\left(l + 1 + \frac{k}{2n}, l + 1, \frac{1}{2} \left(\frac{\xi}{\sigma} \right)^2\right) \\ &\times \left[\sum_{n=0}^{\infty} \frac{1}{n!} \frac{(\epsilon^2 - 2\epsilon)^n}{(1 - \epsilon)^n} \left(\frac{1}{\xi(1 - \epsilon(\xi))} \right)^n \Gamma\left(n + \frac{1}{2}\right) \right. \\ &\times \int_0^{\infty} \exp \left[-\left(\frac{\xi'}{r_0} \right)^{1/n} \right] \xi'^{l+1} \exp \left\{ -\frac{1}{2} \left[\frac{\xi'(1 - \epsilon)}{\sigma} \right]^2 \right\} \\ &\times I_n \left(\frac{\xi(1 - \epsilon(\xi)\xi'(1 - \epsilon))}{\sigma^2} \right) \left. \right]^{-1}, \end{aligned} \quad (10)$$

where $I_n(x)$ are the modified Bessel functions (Abramowitz & Stegun 1964, p. 376).

Fig. 1 shows the radial variation of the ellipticity caused by the seeing. Note how the seeing affects the central points, rounding the isophotes, whereas its effects are progressively less in the outer regions of the profile.

The equations that we have presented for the Sèrsic profiles can be immediately generalized to almost all the experimental profiles (see the theorem in Appendix B).

3 THE EFFECTS OF SEEING ON THE SÈRSIC PROFILE PARAMETERS

3.1 The effect of seeing on the central intensity

To study this effect we use equation (6) and apply the fact that at $\xi = 0$ the confluent hypergeometric function satisfies $M(\mu, \nu; 0) = 1$. This expression can then be written as

$$\begin{aligned} I_c(0) &= I(0)(1 - \epsilon) \sum_{k=0}^{\infty} \frac{(-)^k}{k!} \left(\frac{\sqrt{2}\sigma}{r_0} \right)^{k/n} \Gamma\left(1 + \frac{k}{2n}\right) \\ &\times {}_2F_1\left(\frac{1}{2}, 1 + \frac{k}{2n}; 1; 2\epsilon - \epsilon^2\right), \end{aligned} \quad (11)$$

where ${}_2F_1(a, b; c; z)$ is the hypergeometric function (Abramowitz & Stegun 1964, p. 556).

As shown in Fig. 2, the central intensity of the profile affected by seeing decreases monotonically when the seeing size increases.

The central intensity of profiles with larger values of n decreases more rapidly than for low n as is expected because of the higher central concentration of these profiles.

The central concentration of the object is also dependent on the ellipticity. In Fig. 2 this relation is also shown. Larger ellipticities are more affected by seeing.

3.2 The effect of seeing on the effective radius

The Sèrsic profile can be written in terms of the effective radius and the effective intensity:

$$I(r) = I_e 10^{-b_n[(r/r_e)^{1/n} - 1]}. \quad (12)$$

The constant b_n is chosen such that half the total luminosity predicted by the law comes from $r < r_e$. b_n can be well approximated by the relation $b_n = 0.868n - 0.142$. I_e is the intensity at the effective radius.

The relation between I_e , r_e and $I(0)$, r_0 is given by

$$I(0) = I_e 10^{b_n} \quad (13)$$

and

$$r_0 = (b_n \ln 10)^{-n} r_e. \quad (14)$$

The effect of the seeing on the effective radius can be obtained from the conservation of luminosity by the convolution

$$L^c(r_e^c) = L(r_e), \quad (15)$$

where $L(r_e)$ is the luminosity of the source inside r_e and $L^c(r_e^c)$ is the luminosity obtained from the object affected by seeing, measured inside its effective radius. For a circular object, $\epsilon = 0$, we have

$$L^c(r_e^c) = 2\pi \int_0^{r_e^c} r I_c(r) dr \quad (16)$$

and $L(r_e) = I(0)\pi r_e^2 [n\Gamma(2n)] / [(b_n \ln 10)^{2n}]$ for a Sèrsic profile. Equation (15) can then be written analytically for a circular system as the implicit equation:

$$\begin{aligned} r_e^2 \frac{n\Gamma(2n)}{(b_n \ln 10)^{2n}} &= r_e^{c2} \sum_{k=0}^{\infty} \frac{(-)^k}{k!} \left(\frac{\sqrt{2}\sigma}{r_0} \right)^{k/n} \Gamma\left(1 + \frac{k}{2n}\right) \\ &\times \sum_{l=0}^{\infty} \frac{(-)^l}{l!} \frac{1}{l+1} \frac{(-k/2n)_l}{(1)_l} \left(\frac{r_e^{c2}}{2\sigma^2} \right)^l, \end{aligned} \quad (17)$$

where $(\alpha)_l$ is the Pochhammer symbol: $(\alpha)_l \equiv \Gamma(\alpha + l)/\Gamma(\alpha)$. Fig. 3 shows that the effect of seeing is to increase the effective radius. This effect becomes more important as n increases. The ellipticity effect is also shown; however, for $\epsilon \neq 0$ there is no easy analytical form, so the results with $\epsilon \neq 0$ that are shown in Fig. 3 were obtained numerically. Greater ellipticities imply greater effective radii – these differences are more important for greater values of n . This result is as expected owing to the diminution of the central intensity by the ellipticity effect.

It must be noted that our measurement of effective radius has been obtained over the semimajor axis. Some authors use as the radial distance the magnitude $r^* = \sqrt{ab}$, in this case, the effective radius of the object affected by seeing is given by $r_e^{c*} = r_e^c \sqrt{1 - \epsilon(r_e^c)}$, where $\epsilon(r_e^c)$ can be obtained from equation (9).

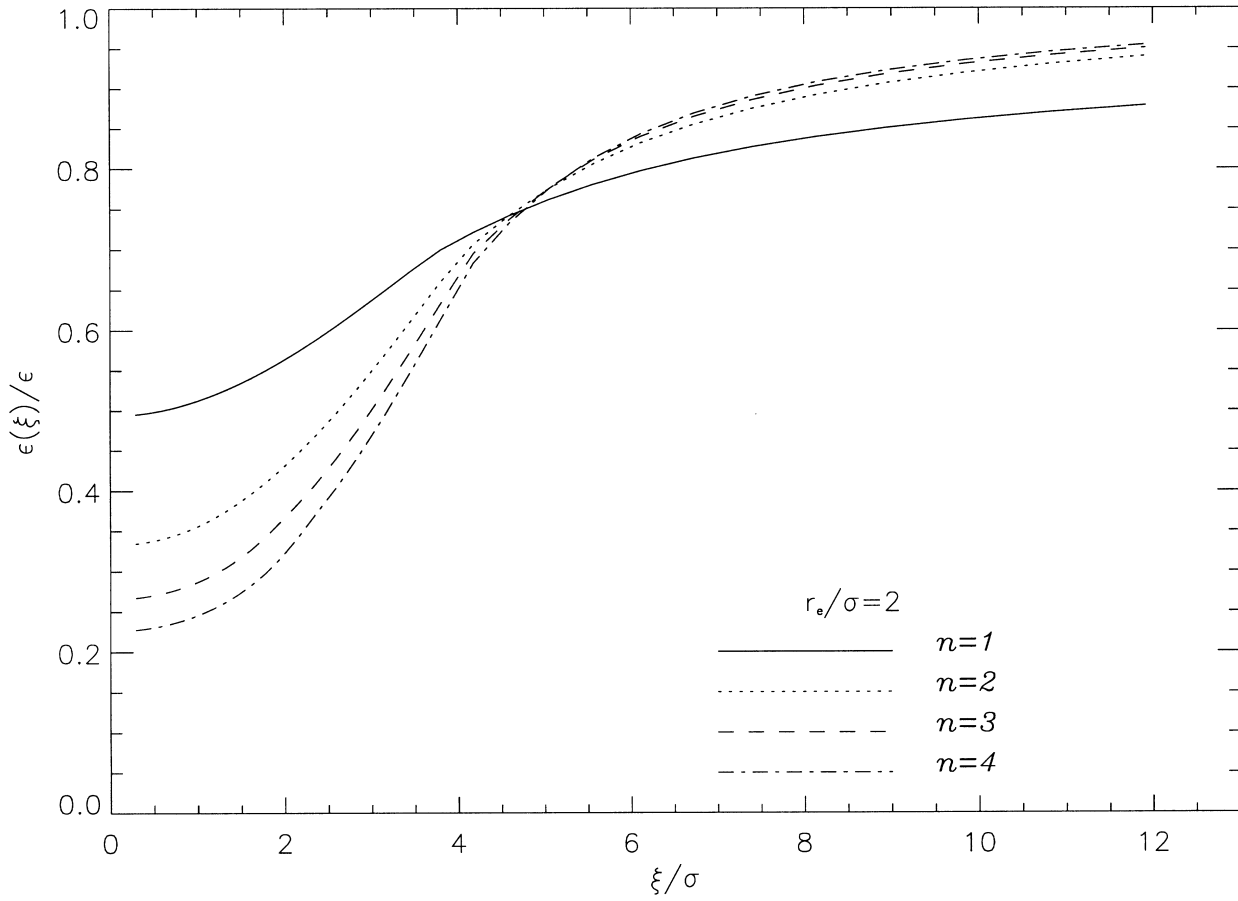


Figure 1. Effects of seeing on the ellipticity. A model with $r_e/\sigma = 2$ is shown.

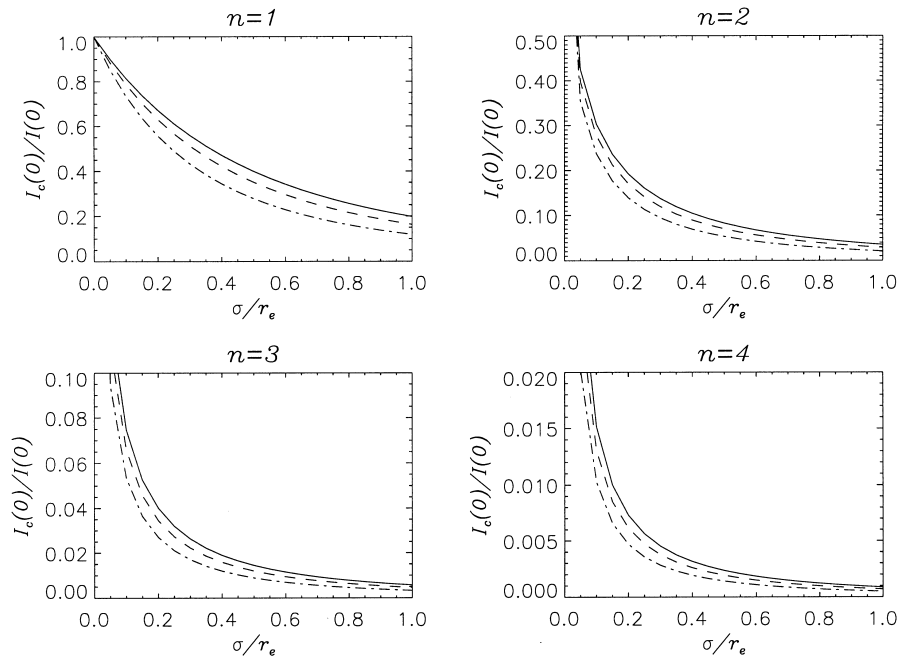


Figure 2. Effects of the seeing on the central intensity $I_e(0)$ for different values of n . Three different ellipticities are shown, $\epsilon = 0$ (full curve), $\epsilon = 0.25$ (broken curve) and $\epsilon = 0.5$ (chain curve).

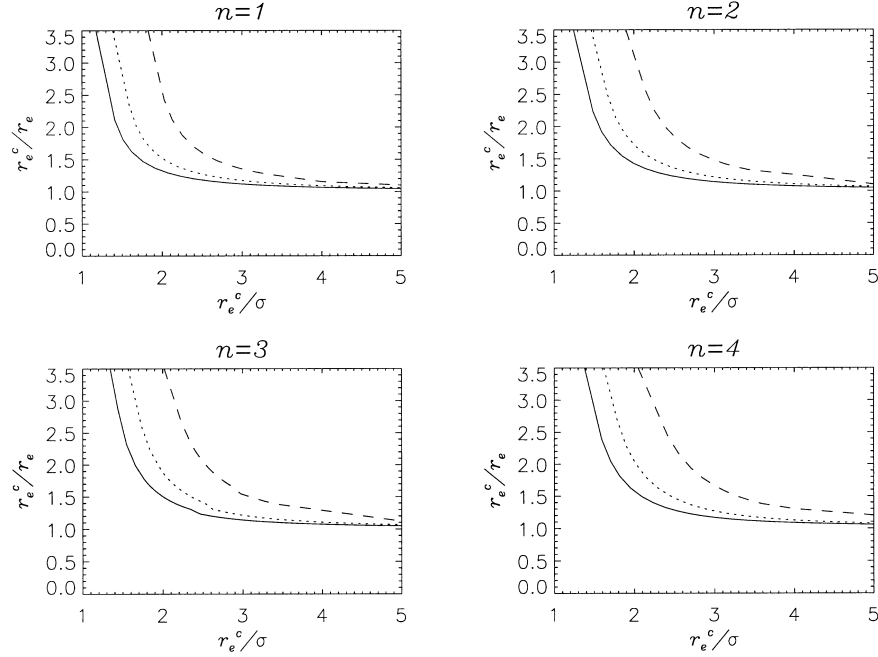


Figure 3. Effects of seeing on the effective radius, r_e^c . Three different ellipticities for the source are shown: $\epsilon = 0$ (full curve), $\epsilon = 0.25$ (dotted curve) and $\epsilon = 0.5$ (broken curve).

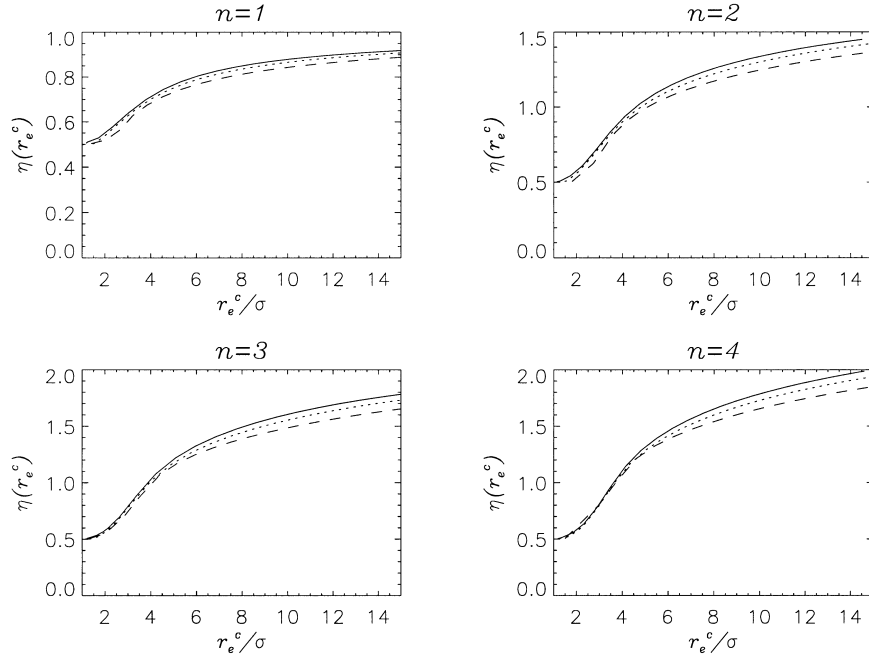


Figure 4. Values of the parameter η at r_e^c as a function of the ratio r_e^c/σ for different values of n and ellipticities: $\epsilon = 0$ (full curve), $\epsilon = 0.25$ (dotted curve) and $\epsilon = 0.5$ (broken curve).

3.3 The effect of seeing on the parameter n

To quantify the effect of seeing on the parameter n we use the parameter

$$\eta(\xi) \equiv \frac{1}{\xi} \frac{I(\xi)}{dI(\xi)/d\xi} \ln \frac{I(\xi)}{I(0)}. \quad (18)$$

This parameter is defined in such a way that $\eta(\xi) = n$ for all

values of ξ if $I(\xi)$ is a Sèrsic profile (equation 5). So $\eta(\xi)$ is equivalent, locally, to the parameter n of the Sèrsic profile. Fig. 4 summarizes the values of this parameter at r_e^c for different n values. It is easy to see that this parameter is the most affected by the seeing. Indeed, $\eta(0) = 0.5$ for any profile affected by a Gaussian seeing. It should be noted that Sèrsic profiles with $n = 0.5$ are Gaussian profiles and then its convolution with a Gaussian PSF gives another Gaussian. The principal conclusion is that seeing effects always produce a surface brightness profile with a

smaller value of n than the actual value. Again, as n increases, the parameter is more affected. The effect of the ellipticity is to decrease the value of n but the changes are not so important.

4 A PRESCRIPTION FOR SEEING CORRECTIONS

Here we present an easy prescription based on the use of the plots of Figs 2–5 (see below). This procedure permits the parameters of the Sersic profile (seeing-free quantities) to be obtained using the observational surface brightness profile. In summary, observers should:

- (i) determine the full width at half-maximum (FWHM) of stars by fitting a Gaussian. σ is related to the FWHM by $\sigma = \text{FWHM}/\sqrt{8 \ln 2}$;
- (ii) measure r_e^c along the semimajor axis solving the implicit equation $L^c(r_e^c) = \frac{1}{2}L^c(\infty)$. This can be done (without any assumptions) directly from the raw images;
- (iii) determine $\eta(r_e^c)$ numerically using the expression

$$\eta(r_e^c) = \frac{1}{r_e^c} \frac{I_c(r_e^c)}{dI_c(\xi)/d\xi|_{r_e^c}} \ln \frac{I_c(r_e^c)}{I_c(0)}; \quad (19)$$

- (iv) evaluate the value of n that corresponds to the point $(\eta(r_e^c), r_e^c/\sigma)$ using Fig. 4. Suppose, as a first approximation, that the value of ϵ corresponds to the value of $\epsilon(r_e^c)$. Note that $\eta(\xi)$ is the parameter less affected by the value of ϵ , so the approximation is good;

- (v) recalculate the value of ϵ more accurately using the value of n obtained and Fig. 5. Fig. 5 shows the values of $\epsilon(r_e^c)$ for different values of n ;

- (vi) obtain the value of r_e using Fig. 3;

- (vii) obtain the value of $I(0)$ using Fig. 2.

Observers wishing to be more precise can use the formulae instead of the figures.

5 DISCUSSION

The study presented here has assumed a Gaussian PSF for the seeing. The real observed PSF is not exactly Gaussian. The theory of atmospheric turbulence predicts the PSF to be the Fourier transform of $\exp[-(kb)^{5/3}]$ (Fried 1966; Woolf 1982), where b is a scaling parameter. Saglia et al. (1993) generalized this result, they assume a PSF that is the Fourier transform of $\exp[-(kb)^\gamma]$. The Gaussian PSF is a particular case with $\gamma = 2$. Their observational PSFs were in agreement with the theoretical PSF inferred by the turbulence theory. They obtain a Gaussian FWHM that is 4.67 per cent greater than the FWHM of the turbulence PSF with $\gamma = 5/3$. This systematic error will be transmitted into the parameters I_e , r_e and n . We have computed these parameters, varying σ in our PSF by 4.67 per cent, and have found that I_e is underestimated by 7 per cent, r_e is overestimated by 7 per cent and n is underestimated by 4 per cent in a systematic manner with respect to the initial values. Owing to the systematic character of these errors they can be easily taken into account.

The parameter most affected by the seeing is n . This has important consequences because n serves to classify the type of profile and is related to the central luminosity concentration. Graham et al. (1996) and Jerjen, Bingelli & Freeman (2000) found a correlation between n and the galactic type. Thus, dwarfs ellipticals show the smallest values of n and cD galaxies have the largest values. Between these extremes are located the ellipticals and the bulges of spirals. The parameter $\eta(\xi)$ defined in Section 3.2 gives information locally concerning the value of n over the profile. Fig. 4 shows $\eta(r_e^c)$ for different values of the seeing. It can be observed that the seeing always produces $\eta(r_e^c) < n$ for all the values of the r_e^c/σ ratio. If seeing is not taken into account, the value of n that can be measured from the profiles is always smaller than the real one. Usually, fitting procedures avoid the central points in order to remove seeing effects from the profiles. This is clearly not sufficient to recover the real value of n (see Fig. 4).

One physical restriction to the values of n is given by the luminosity density. For a homologous triaxial ellipsoid, the

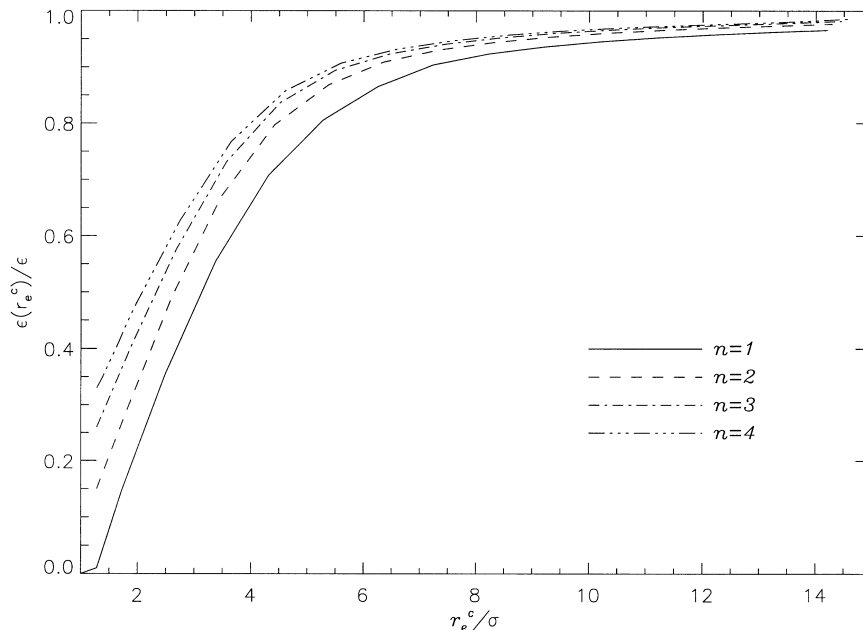


Figure 5. Values of the ellipticity of the isophotes at r_e^c as function of the ratio r_e^c/σ for different values of n .

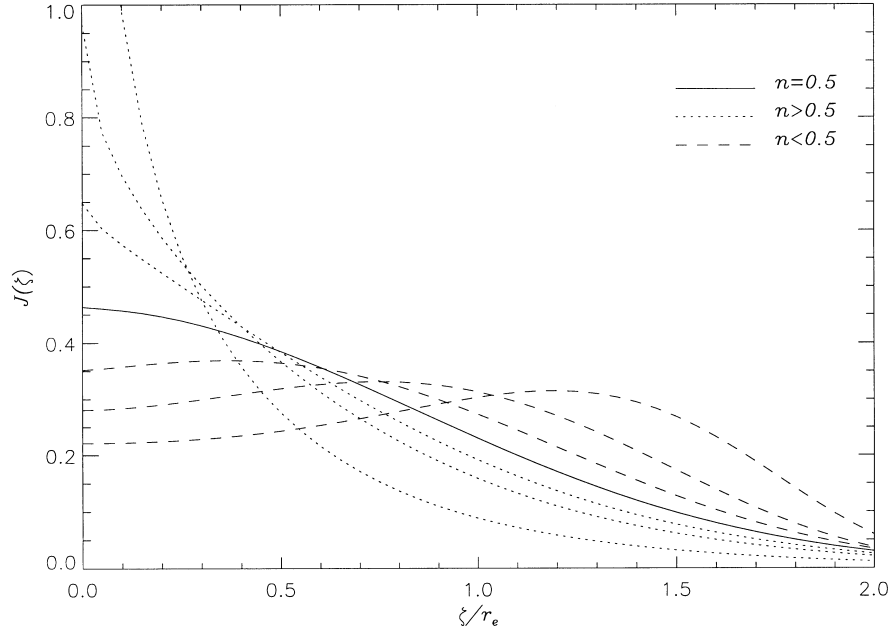


Figure 6. Normalized luminosity density $J(\xi) = j(\xi)r_e^{1/n}/[f^{1/2}I(0)]$ versus the radial coordinate ξ/r_e for Sèrsic profiles with $n < 1$: $n = 0.2, 0.3$ and 0.4 (broken curves), $n = 0.5$ (full curve) and $n = 0.7, 0.8$ and 1.0 (dotted curves).

luminosity density (Stark 1977) associated with a Sèrsic profile is given by

$$j(\xi) = \frac{f^{1/2}}{\pi} \frac{K}{n} \frac{I(0)}{r_e^{1/n}} \int_{\xi}^{\infty} \exp \left[-K \left(\frac{\xi}{r_e} \right)^{1/n} \right] \xi^{1/n-1} (\xi^2 - \xi_e^2)^{-1/2} d\xi, \quad (20)$$

where $K = b_n \ln 10$ and $f^{1/2}$ is a constant that depends on the three-dimensional (3D) spatial orientation of the object. We have calculated the luminosity density for Sèrsic profiles with $n < 1$ (see Fig. 6). For $n < 0.5$ the density has a depression in its central parts. This represents an unlikely physical situation. Nevertheless, the seeing effects prevent the measurement of $n < 0.5$ for objects with $n \geq 0.5$ (see Fig. 4).

The effects of seeing on the parameters I_e , r_e and n depend on the intrinsic ellipticity (ϵ) of the source. Thus, assumes that the object has $\epsilon = 0$, when it really is elliptical-symmetric, resulting in the central intensity and n begin underestimated, whereas r_e is overestimated. These effects are not negligible and they are more important when ϵ increases.

6 CONCLUSIONS

We have developed an analytical study of the seeing effects on Sèrsic profiles. The seeing PSF was modelled by a Gaussian function. In this analysis we have taken into account the intrinsic ellipticity of the objects. Our main results are the following.

(i) The convolved surface brightness profile along the major axis of the object can be expressed as a double series of confluent hypergeometric functions. This result is very general and can be applied to nearly all the experimental surface brightness profiles.

(ii) We have obtained an implicit equation to evaluate the effect of seeing on the ellipticity of the isophotes. The rounding of the isophotes depends on n , r_e , σ and ϵ in a unique way.

(iii) The parameter most affected by the seeing effect is n . The

observed Sèrsic profiles show smaller values of n , because of the seeing effect, than the real ones. Greater values of n are the most affected. Also, for $n < 0.5$, the luminosity density associated with a Sèrsic profile has a depression in its central parts. This represents an unlikely physical situation.

(iv) The seeing effects on the parameters of the Sèrsic profile depend on the intrinsic ellipticity of the object, therefore it is necessary to include it when seeing effects are studied.

The results described here clearly show that seeing effects are important when one tries to measure accurate values of the parameters of a profile affected by the seeing. These results have to be taken into account for sources with a low r_e/σ relation as expected for medium- and high-redshift objects.

ACKNOWLEDGMENTS

We wish to thank J. A. Rubiño for valuable discussions and E. Simmoneau for useful comments. We are also indebted to V. Debattista who kindly read versions of this manuscript. JALA was supported by grant 20-56888.99 from the Schweizerischer Nationalfonds.

REFERENCES

- Abramowitz M., Stegun I., 1964, Handbook of Mathematical Functions. Dover, New York
- Andredakis Y., Peletier R., Balcells M., 1995, MNRAS, 275, 874
- Caon N., Capaccioli M., D'Onofrio M., 1993, MNRAS, 265, 1013
- Davies J., Philips S., Cawson M., Disney M., Kibblewhite E., 1988, MNRAS, 232, 239
- de Vaucouleurs G., 1948, Ann. Astrophys, 11, 247
- Franx M., Illingworth G., Heckman T., 1989, AJ, 98, 2
- Freeman K., 1966, MNRAS, 133, 47
- Fried D. L., 1966, J. Opt. Soc. Am., 56, 1372
- Graham A., Lauer T., Colles M., Postman M., 1996, ApJ, 465, 534
- Hubble E., 1930, ApJ, 71, 231

- Hubble E., 1936, *The Realm of the Nebulae*, Yale Univ. Press. New Haven, CT
- Jerjen E., Bingelli B., Freeman K., 2000, *AJ*, 119, 523
- King I. R., 1971, *PASP*, 83, 199
- Moffat A. F. J., 1969, *A&A*, 3, 455
- Prieto M., Aguerri J. A. L., Varela A. M., Munoz-Tunón C., 2000, *A&A*, in press
- Saglia R., Bertschinger E., Baggle G., Burstein D., Colles M., Davies R., McMahon R., Wegner G., 1993, *MNRAS*, 264, 961
- Sèrsic J., 1968, *Atlas de Galaxias Australes* Córdoba: Obs. Astronómico
- Stark A., 1977, *ApJ*, 213, 368
- Schweizer F., 1979, *ApJ*, 223, 23
- Woolf N. J., 1982, *ARA&A*, 20, 367

APPENDIX A: ANALYTICAL EXPRESSION ON MINOR AXIS

Using equation (3) we can also obtain the equation for the minor axis, $\theta = \pi/2$,

$$I_c\left(\xi, \frac{\pi}{2}\right) = \frac{I(0)}{\pi^{1/2}} \frac{1}{(1-\epsilon)} \exp\left\{-\frac{1}{2} \left[\frac{\xi(1-\epsilon)}{\sigma}\right]^2\right\} \\ \times \sum_{k=0}^{\infty} \frac{(-)^k}{k!} \left[\frac{\sqrt{2}\sigma}{r_0(1-\epsilon)}\right]^{k/n} \\ \times \sum_{l=0}^{\infty} \frac{1}{l!} \left[\frac{\epsilon^2 - 2\epsilon}{(1-\epsilon)^2}\right] \frac{\Gamma\left(l + \frac{1}{2}\right)}{\Gamma(l+1)} \Gamma\left(l + 1 + \frac{k}{2n}\right) \\ \times M\left(l + 1 + \frac{k}{2n}, l + 1, \frac{1}{2} \left[\frac{\xi(1-\epsilon)}{\sigma}\right]^2\right). \quad (\text{A1})$$

However, this expression is divergent for $|(\epsilon^2 - 2\epsilon)/(1-\epsilon)^2| > 1$, so that for $\epsilon \geq 0.3$ the use of the integral expression is required:

$$I_c\left(\xi, \frac{\pi}{2}\right) = \frac{1}{2\pi\sigma^2} (1-\epsilon) \exp\left[-\frac{1}{2} \frac{(1-\epsilon)^2 \xi^2}{\sigma^2}\right] \\ \times \int_0^{\infty} \xi' d\xi' I(\xi') \exp\left[-\frac{1}{2} \frac{(1-\epsilon)^2 \xi'^2}{\sigma^2}\right] \\ \times F_2(\xi, \xi', \sigma, \epsilon), \quad (\text{A2})$$

where $F_2(\xi, \xi', \sigma, \epsilon)$ is given by

$$F_2(\xi, \xi', \sigma, \epsilon) = 2\pi^{1/2} \left\{ \pi^{1/2} I_0\left(\frac{\xi\xi'}{\sigma^2}\right) + \sum_{n=1}^{\infty} \frac{1}{n!} \frac{(\epsilon^2 - 2\epsilon)^n}{(1-\epsilon)^{2n}} \left(\frac{\xi'}{\xi}\right)^n \right. \\ \left. \times \Gamma\left(n + \frac{1}{2}\right) I_n\left[\frac{\xi\xi'}{\sigma^2}(1-\epsilon)^2\right] \right\}. \quad (\text{A3})$$

In the limiting cases, $\xi \rightarrow \infty$ or $\sigma \rightarrow 0$, for $\epsilon < 0.3$, the

asymptotic expression of the confluent hypergeometric function (Abramowitz & Stegun 1964) can be used again to recover the original Sèrsic expression:

$$I_c\left(\xi, \frac{\pi}{2}\right) = I(0) \exp\left[-\left(\frac{\xi}{r_0}\right)^{1/n}\right] \\ \times \left[1 + O\left(\left[\frac{\xi^2}{2\sigma^2}(1-\epsilon)^2\right]^{-1}\right)\right]. \quad (\text{A4})$$

APPENDIX B: THEOREM ON GAUSSIAN SEEING

Assume a surface brightness distribution with elliptical symmetry, $I(\xi)$. If this distribution can be written as the power series

$$I(\xi) = I(0) \sum_{k=0}^{\infty} \alpha(k) \xi^{\beta k}, \quad (\text{B1})$$

with a region of convergence equal to $0 \leq \xi < \infty$, then the analytical solution of the convolution of $I(\xi)$ with a Gaussian PSF over the major axis is

$$I_c(\xi, 0) = \frac{I(0)}{\pi^{1/2}} (1-\epsilon) \exp\left[-\frac{1}{2} \left(\frac{\xi}{\sigma}\right)^2\right] \sum_{k=0}^{\infty} \alpha(k) (\sqrt{2}\sigma)^{\beta k} \\ \times \sum_{l=0}^{\infty} \frac{1}{l!} (2\epsilon - \epsilon^2)^l \frac{\Gamma\left(l + \frac{1}{2}\right)}{\Gamma(l+1)} \Gamma\left(l + 1 + \frac{\beta k}{2}\right) \\ \times M\left(l + 1 + \frac{\beta k}{2}, l + 1, \frac{1}{2} \left(\frac{\xi}{\sigma}\right)^2\right). \quad (\text{B2})$$

For $\epsilon = 0$, the convolution can be written as

$$I_c(\xi) = I(0) \exp\left[-\frac{1}{2} \left(\frac{\xi}{\sigma}\right)^2\right] \sum_{k=0}^{\infty} \alpha(k) (\sqrt{2}\sigma)^{\beta k} \Gamma\left(1 + \frac{\beta k}{2}\right) \\ \times M\left(1 + \frac{\beta k}{2}, 1, \frac{1}{2} \left(\frac{\xi}{\sigma}\right)^2\right). \quad (\text{B3})$$

For the Sèrsic profile, $\alpha(k) = [(-)^k/k!](1/r_0)^{k/n}$, $\beta = 1/n$.

Examples of profiles where the theorem is not applicable are the Hubble profile (Hubble 1930) and the Freeman bar profile (Freeman 1966). The first one does not admit a convergent power series over the entire interval of definition, and the second one has a point of non-differentiability that avoids a power-series expansion.

This paper has been typeset from a $\text{\TeX}/\text{\LaTeX}$ file prepared by the author.